

Astronomy & Astrophysics manuscript no.
(will be inserted by hand later)

Fireballs from Quark Stars in the CFL Phase

Application to Gamma Ray Bursters

R. Ouyed¹, R. Rapp², and C. Vogt³

¹ Department of Physics and Astronomy, University of Calgary, Calgary, Canada

² Cyclotron Institute and Physics Department, Texas A&M University, College Station, TX 77843-3366, USA

³ Nordic Institute for Theoretical Physics, Blegdamsvej 17, DK-2100 Copenhagen, Denmark

Received/Accepted

Abstract. Recent studies of photon-generation mechanisms in the color-superconducting Color-Flavor Locked (CFL) phase of dense quark matter have found γ -ray emissivities in excess of $\sim 10^{50} \text{ erg cm}^{-3} \text{ s}^{-1}$ for temperatures in the 10-30 MeV range. We suggest that this property can trigger γ -ray bursts (GRBs) and associated fireballs at the surface of hypothetical hot (newly born) quark stars with an energy release of up to $10^{48} - 10^{50} \text{ erg}$ within a fraction of a millisecond. If surrounded by an accretion disk following its formation, the star's bursting activity can last from tens of milliseconds to hundreds of seconds releasing up to 10^{52} erg in total energy. We discuss typical features of observed GRBs within our model and explain how quark stars in the CFL phase might constitute natural candidates for corresponding inner engines.

Key words. dense matter – Gamma rays: bursts – stars: evolution – stars: interior

1. Introduction

Nuclear matter at high density and small temperature (T) is expected to exhibit color-superconductivity (CSC), induced by quark pairing and condensation at the Fermi surface, with energy gaps $\Delta \simeq 100 \text{ MeV}$ (Rapp, Schäfer, Shuryak, & Velkovsky 1998; Alford, Rajagopal, & Wilczek 1998) and associated critical temperatures $T_c \simeq 0.6\Delta$, above which thermal fluctuations destroy the condensate (for a review, see, e.g., Rajagopal & Wilczek 2000). The experimental relevance of such matter mostly pertains to astrophysical objects, in particular compact stars. Besides its impact on the equation of state (Lugones & Horvath 2002, Alford & Reddy 2003), CSC could affect the emission spectrum of compact stars as encoded in its electroweak properties (Jaikumar, Prakash, & Schäfer 2002; Reddy, Sadzikowski, & Tachibana 2003; Vogt, Rapp, & Ouyed 2004). If CSC extends to the surface of a hypothetical quark star, pulsed photon emission has been suggested as a mechanism for a fireball in the γ -ray burst (GRB) context for the 2-flavour superconductor (2SC) in (Ouyed & Sannino, 2002)¹. Whereas at moderate densities

(and $T=0$) the existence of the 2SC is still under debate (Alford & Rajagopal, 2002; Buballa et al. 2004) – it could be superseeded by, e.g., crystalline phases (Alford, Bowers, & Rajagopal, 2001; Rapp, Shuryak, & Zahed, 2001) –, the Color-Flavor Locked (CFL) phase is the favored ground state at sufficiently high density (Alford, Rajagopal & Wilczek, 1999). In CFL matter all three quark flavours (up, down and strange) have a mass which is negligible compared to the (quark) chemical potential, μ_q , so that they participate equally in the color condensation, breaking the full (local) color-symmetry and one (global) $SU(3)$ chiral symmetry. Therefore, the zero-temperature CFL phase is electrically neutral without electrons, colorless, and its low-lying excitations are characterised by 8+1 Goldstone bosons (due to chiral and baryon-number symmetry breaking).

In previous work (Vogt, Rapp, & Ouyed, 2004), hereafter VRO, we have explored photon emission and absorption mechanisms in the CFL phase. Based on the Goldstone boson excitations (“generalised pions”) of the broken chiral symmetry we have employed a Hidden Local Symmetry formalism including vector mesons (“generalised ρ -mesons”) to assess photon production rates and mean free paths at temperatures suitable for CFL. We have found that above $T \simeq 5-10 \text{ MeV}$, the emissivities from pion annihilation, $\pi^+\pi^- \rightarrow \gamma\gamma$ and $\pi^+\pi^- \rightarrow \gamma$ (rendered possible due to an in-medium pion dispersion relation), dominate over those from conventional electro-

Send offprint requests to: ouyed@phas.ucalgary.ca

¹ In the 2SC phase, up and down quarks pair into a color-antitriplet, leaving the quarks of the remaining color unpaired, and with five of the eight gluons acquiring a mass. The 3 massless gluons possibly bind into light glueballs subject to fast decays into photons (Ouyed & Sannino 2001).

magnetic annihilation, $e^+e^- \rightarrow \gamma\gamma$. According to Fig. 2 of VRO, the photon emissivity can be as high as $10^{50} - 10^{53}$ erg cm $^{-3}$ s $^{-1}$ for $T \simeq 10\text{-}30$ MeV. The objective of the present article is to (i) investigate the astrophysical consequences of such photon production mechanisms² for the early cooling history of hot CFL stars (Sect. 2) and (ii) evaluate whether the resulting fireballs can drive/power GRBs (Sect. 3). Conclusions are given in Sect. 4.

2. Early Cooling of CFL stars

2.1. Plasma photon attenuation

The surface emissivity of photons with energies below $\hbar\omega_p \simeq 23$ MeV (ω_p : electromagnetic plasma frequency) is strongly suppressed (Alcock, Farhi, & Olinto 1986; Chmaj, Haensel, & Słomiński 1991; Usov 2001). As shown in VRO, average photon energies in CFL matter at temperature T are $\sim 3T$. Therefore, as soon as the surface temperature of the star cools below $T_a = \hbar\omega_p/3 \simeq 7.7$ MeV, we consider the photon emissivity to be shut off (“attenuated”), i.e., photon emission only lasts as long as the star cools from its initial temperature T_0 to T_a . With this in mind we proceed to study the thermal evolution of the star.

2.2. Heat transfer and thermal evolution

We describe the thermal evolution by a diffusion equation,

$$c_v \frac{\partial T}{\partial t} = \frac{1}{r^2} \frac{\partial}{\partial r} \left(r^2 \kappa \frac{\partial T}{\partial r} \right), \quad (1)$$

where c_v and κ are the specific heat and thermal conductivity of the star matter, respectively. In the CFL phase, these are dominated by massless Goldstone bosons, as evaluated in Jaikumar et al. (2002),

$$c_v = \frac{2\sqrt{3}\pi^2}{5} T^3 = 7.8 \times 10^{16} T_{\text{MeV}}^3 \text{ erg cm}^{-3} \text{ K}^{-1}, \quad (2)$$

and in Shovkovy & Ellis (2002),

$$\kappa = 1.2 \times 10^{27} T_{\text{MeV}}^3 \lambda_{GB} \text{ erg cm}^{-1} \text{ s}^{-1} \text{ K}^{-1} \quad (3)$$

with a Goldstone-boson mean free path (in [cm] in Eq. (3))

$$\lambda_{GB}(T) = \frac{4(21 - 8 \ln 2)}{15\sqrt{2}\pi T_{\text{MeV}}} \exp \left(\sqrt{\frac{3}{2}} \frac{\Delta_{\text{MeV}}}{T_{\text{MeV}}} \right) \text{ cm}. \quad (4)$$

Effects of a crust have been ignored in the present study of the star’s cooling history (see discussion in § 3.4).

² We note that our study is different from those involving the e^+e^- emission above the surface of CFL stars (see, e.g., Page & Usov 2002 and references therein). The latter scenarios reside on the fact that the color-superconductive matter of the star carries a charge so that an e^- abundance can build up thereby generating a critical electric field that in turn produces and emits e^+e^- pairs and photons. This is quite different from our model which is based on photon generation inside the star with negligible (e^+e^-) emission.

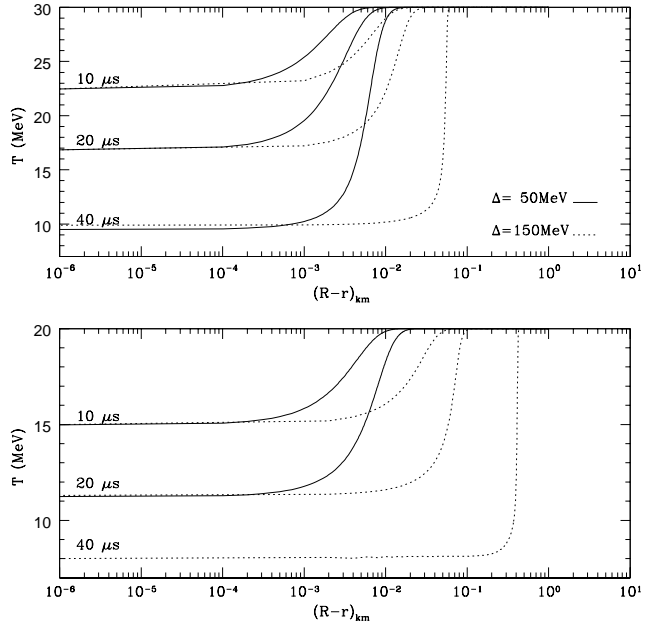


Fig. 1. Radial temperature profiles of CFL stars of radius R according to solutions of the diffusion Eq. (1) (r : distance to the star’s center) for two different gaps, $\Delta=50$ MeV (solid lines) 150 MeV (dotted lines), and initial temperatures $T_0=30$ MeV (upper panel) and 20 MeV (lower panel). In the lower panel, the $\Delta=50$ MeV case cools to $T_a=7.7$ MeV (lower limit of the plots) in less than 40 μ s.

In dimensionless units, the diffusion equation becomes

$$\frac{\partial \tilde{T}^4}{\partial \tau} = \frac{\alpha}{\tilde{r}^2} \frac{\partial}{\partial \tilde{r}} \left(\tilde{\lambda}_{GB} \tilde{r}^2 \frac{\partial \tilde{T}^4}{\partial \tilde{r}} \right) \quad (5)$$

with $\tilde{r} = r/R$, $\tilde{T} = T/T_0$, $\tau = t/(R/c)$, $\tilde{\lambda}_{GB} = \lambda_{GB}/R$ and a numerical coefficient $\alpha=0.512$ (c is the speed of light). As initial condition we assume the temperature of the star at $\tau = 0$ be uniform, $\tilde{T}(\tau = 0) = \tilde{T}_0$. We further have to impose boundary conditions for the temperature gradient in terms of the heat flux, $F(\tilde{r}) = -\tilde{\lambda}_{GB} \partial \tilde{T} / \partial \tilde{r}$, at the center and the surface of the star, $F(\tilde{r} = 0) = 0$ and $F(\tilde{r} = 1) = \tilde{T}^4$. Due to the large opacity we expect that the photons to be thermalised upon leaving the star. Thus, we assume black-body radiation to be a good approximation (supported by VRO). The energy flux per unit time through a spherical shell at a radius \tilde{r} is evolved by taking into account the gradient of temperature on both sides of the shell. For the outermost shell, the flux exits the star via thermal photons, implying that the cooling curves result from photon emission only.

Numerical solutions to Eq. (5), using a finite-difference method, are summarized in Figs. 1 and 2 for a quark star of radius $R=10$ km. Fig. 1 shows the temperature vs. distance from the star’s surface, $R-r$, indicating that T drops to T_a in less than 0.1 ms over a shell of thickness less than ~ 1 km. Neglecting heat transport, the cooling timescale

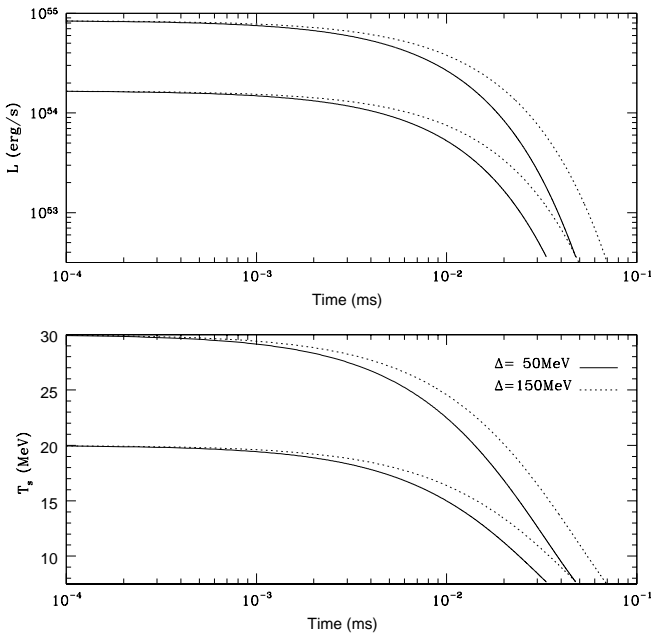


Fig. 2. Time dependence of surface temperature (lower panel) and photon luminosity (upper panel) of a CFL star for two initial temperatures, $T_0=20$ and 30 MeV (lower and upper lines, respectively). Solid (dotted) lines are for $\Delta=50(150)$ MeV.

may be roughly estimated from $c_v(\partial T/\partial t)=-\epsilon=-L/\Delta V$ ($\Delta V=4\pi R^2\Delta R$: volume of the cooling shell of thickness ΔR). Assuming a blackbody luminosity, $L=4\pi R^2\sigma T^4$, one finds $t_{\text{cool}} \simeq 0.1\text{ms} \times \Delta R_{\text{km}} \times (\Delta T/T)$, ($\Delta T = T_0 - T_a$), approximately reflecting the numerical results. Note that our estimate improves toward small T and large Δ for which λ_{GB} is larger, so that neglecting the delay time due to heat transport (Eq. (1)) is better justified; e.g., for $T_0=20$ MeV and $\Delta=150$ MeV (in which case $\lambda_{GB}=10^{-2}\text{km}$, reaching 1 km at $T \simeq 15$ MeV), $\Delta R_{\text{km}} \simeq 1$ (lower panel in Fig. 1); with $(\Delta T/T) \simeq 1$ one recovers $t_{\text{cool}} \simeq 0.1$ ms, consistent with the lower panel of Fig. 2.

For identical T_0 , a larger gap implies cooling deeper into the star, but slower in terms of the reduction in surface temperature, cf. Fig. 2. Again, this follows from the larger λ_{GB} , for which heat emerges from deeper in the star and thus provides a larger energy reservoir.

When increasing the initial temperature, T_0 , from 20 MeV to 30 MeV, the surface cooling does not change radically. The main difference is that the cooling of the bulk sets in earlier so that the temperature gradient between surface and bulk is washed out in shorter time.

We recall that contributions from neutrino (ν) emission are not included in our analysis. We expect this to be a reasonable approximation since (i) ν emission from the surface is usually negligible in comparison to photon emission in the temperature region we are considering (see also VRO for more details), and (ii) ν emission from the bulk will set in once the neutrino mean-free-path becomes com-

parable to the star radius which is expected to occur for temperatures below ~ 5 MeV (Reddy et al. 2002); above, the neutrinos are essentially trapped inside the star.

We also note that photons will be redshifted as they stream outwards due to the star's gravitational potential. First order General Relativity effects on the emissivities can be introduced through redshift factors expressed in terms of the star mass and radius. We estimate the pertinent redshift reduction to be of the order of 10% (cf. Frolov & Lee 2005 for a recent analysis). While the gravitational redshift will degrade the total energy emitted it should not affect the qualitative features of our results.

3. Application to Gamma Ray Bursts

The total energy released during cooling is computed from Fig. 2 as $E_{\text{tot}} = \int L_{\gamma} dt$. Thus, a CFL star with initial temperature of 10-30 MeV can release on average 10^{48} - 10^{50} erg within ~ 0.1 ms as it cools to T_a . We have at hand an engine that could be driving observed GRBs.

3.1. Accretion disk and temporal variability

Our main idea for the following is that the input energy to the engine is provided by infalling matter from an accretion disk. The energy released by the hot CFL star translates into $(0.01 - 1)M_{\odot}c^2 \text{ s}^{-1}$ in accretion energy. These values are reminiscent of hyperaccreting disks (Popham, Woosley, & Fryer 1999) suggesting that if the latter is indeed formed around a CFL star it could reheat the surface of the star via accretion keeping the engine active for a much longer time and providing higher energies as compared to collapse events only. More precisely, the total available energy is related to the disk mass, M_{disk} , by

$$E_{\text{T}} \simeq \eta M_{\text{disk}}c^2 + \frac{M_{\text{disk}}}{m_{\text{H}}} \Delta E_{\text{B}} , \quad (6)$$

where the first term accounts for the release in gravitational binding energy of the accreted matter, with $\eta \sim 0.1$ (e.g., Frank, King, & Raine 1992). The second term represents the binding energy released in the conversion from nuclear to CFL matter (ΔE_{B} per nucleon). It is presumably emitted via neutrinos (Glendenning 1997) so that $E_{\text{T}} \simeq \eta M_{\text{disk}}c^2$ remains available to photon production.

We are modelling the effects of the accreted material on the CFL star in a very simplistic approach, as a random increase of the CFL surface temperature T_s (heating) to a value T_{peak} with a uniform distribution between the lower limit, $T_a \simeq 7.7$ MeV, and an upper limit, $T_{\text{max}} = 15$ - 30 MeV. This roughly corresponds to expected average disk temperatures up to $T_{\text{disk}} \simeq 15$ MeV or so (Popham et al. 1999); we neglect cooling processes during accretion. Note that for accreted material with temperature below T_a there is no bursting and the engine remains shut off until further accretion drives T_s above T_a . In these cases the accretion proceeds for longer than the average accretion timescale.

For the time intervals of accretion, Δt_{accr} , we assume the free-fall time for a hyperaccreting disk as the relevant

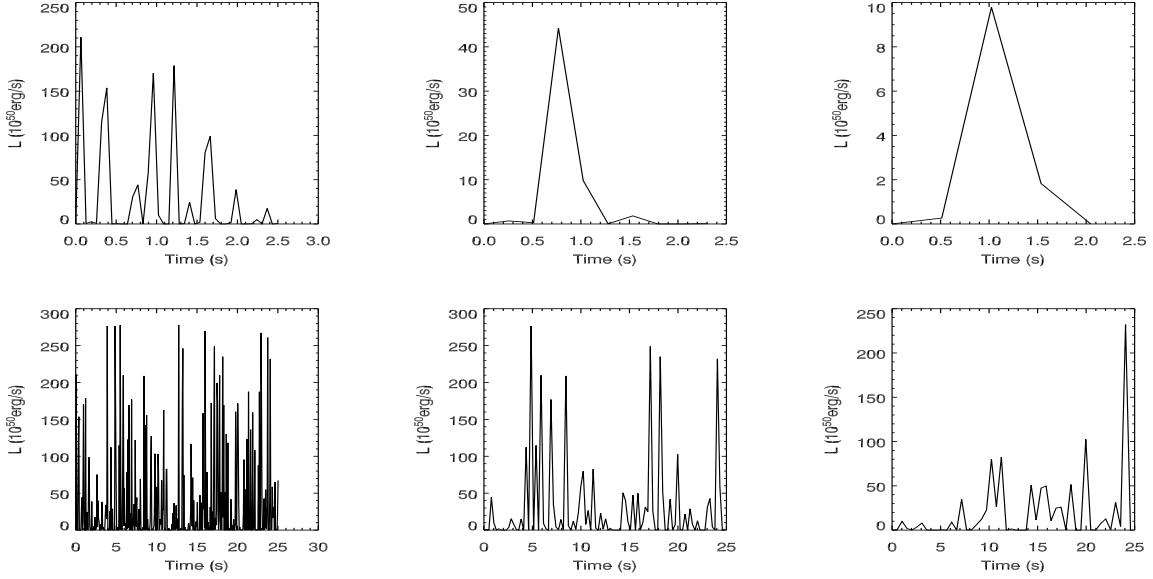


Fig. 3. Model results for the effects of a hyperaccreting disk on the star luminosity; shown is the γ -ray burst emission versus time for three different time resolutions (64 ms, 256 ms, and 512 ms from left to right) representative of GRBs detectors (www.batse.msfc.nasa.gov/batse/grb/lightcurve/). The upper (lower) panels are for a total accreted energy $E_T=0.001M_\odot c^2$ ($E_T=0.01M_\odot c^2$) with $T_{\max}=30$ MeV.

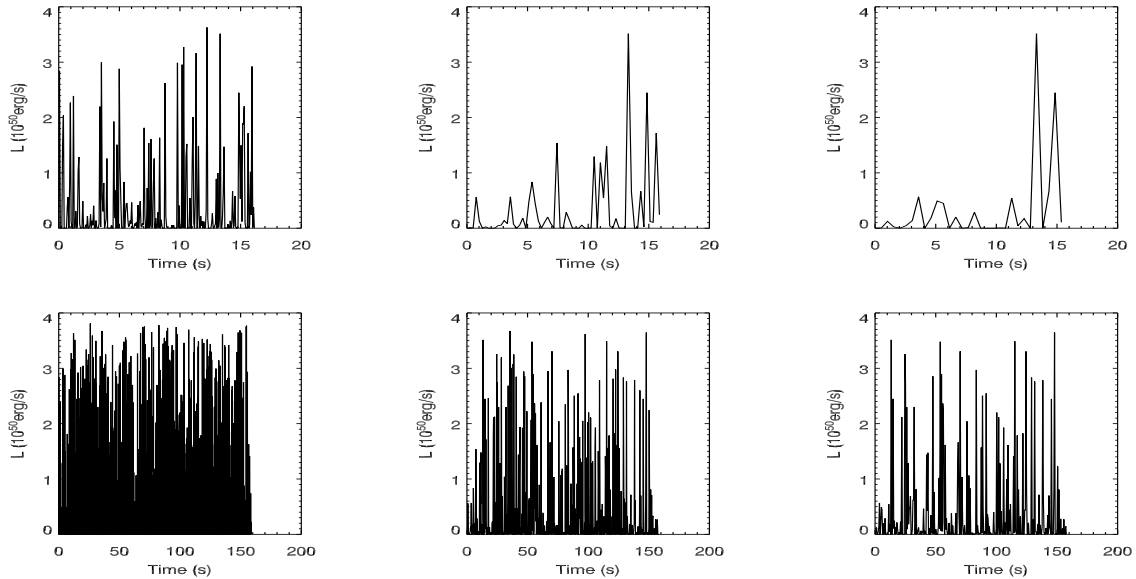


Fig. 4. Same as in Fig. 3 but for $T_{\max}=20$ MeV. More sample of lightcurves can be found at <http://www.capca.ucalgary.ca/>.

scale, $t_{\text{ff}}=1/\sqrt{4\pi G\rho_{\text{disk}}}\simeq 1$ ms, with $\rho_{\text{disk}}\simeq 10^{12}$ g cm $^{-3}$ the accretion disk density and G the gravitational constant. The accretion time intervals are sampled stochastically between 1 and 10 ms. The time scale, Δt_γ , of the subsequent γ -ray burst (cooling) follows from the diffusion Eq. (5) as the time it takes to cool the surface to T_a . During this time the accretion energy is transformed to photon energy which in a simple form can be written as $L_\gamma\Delta t_\gamma=\eta M_{\text{disk}}c^2\Delta t_{\text{accr}}$. Thus, each event (reheating and cooling) lasts for $\Delta t_{\text{event}}=\Delta t_{\text{accr}}+\Delta t_\gamma$, for given Δ and

T_{peak} (we set $\Delta=50$ MeV). Consequently, each episode lasts for a few milliseconds consisting of a linear increase of T_s to T_{peak} followed by a rather sharp decrease to T_a .

For a given disk mass (see § 3.5), the simulation is carried out until the total available energy, $E_T\simeq 0.1M_{\text{disk}}c^2$ (Eq. (6)), is consumed. The resulting variability (displayed in Figs. 3 and 4 for $E_T=0.001M_\odot c^2$, $0.01M_\odot c^2$ and typical time resolutions of GRB detectors) share interesting similarities to those observed in GRB data, see, e.g., <http://www.batse.msfc.nasa.gov/grb/lightcurve>.

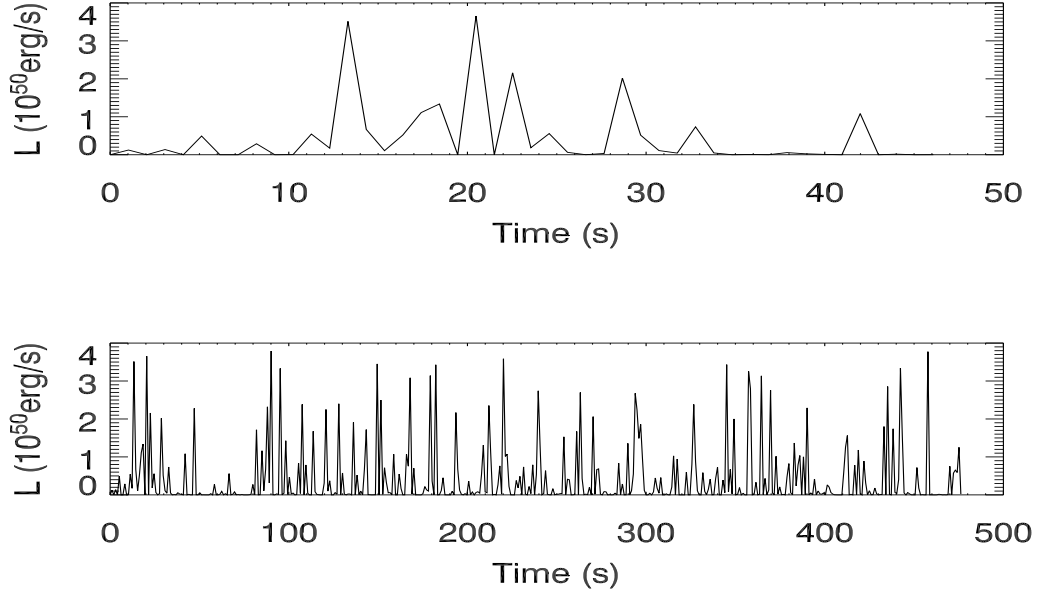


Fig. 5. γ -ray burst emission spectra versus time for a CFL star with accretion disk of mass $0.01M_{\odot}$ (or $E_T = 0.001M_{\odot}c^2$; upper panel) and $0.1M_{\odot}$ (or $E_T = 0.01M_{\odot}c^2$; lower panel), with $T_{\max}=15$ MeV and time resolution 1024 ms. More examples can be found at <http://www.capca.ucalgary.ca/>.

Note that our spectra correspond to the activity directly at the engine while the GRB curves represent emission beyond the transparency radius (see, e.g., Piran 2000). Nevertheless, the engine activity should reflect the variability at large distances.

3.2. Total duration

Our simulations of the accretion suggest engine activities varying from milliseconds to hundreds of seconds depending on M_{disk} and T_{\max} (Figs. 3 and 4). The average duration can be estimated as $t_{\text{dur}} \simeq \Delta\bar{t}_{\text{accr}} \times (E_T/\bar{E}_{\gamma})$ with average burst energy and accretion timescale $\bar{E}_{\gamma} \simeq 10^{49}$ erg and $\Delta\bar{t}_{\text{accr}} \simeq 5$ ms, respectively. One obtains $t_{\text{dur}} \simeq 10$ s for a CFL star surrounded by a $0.1M_{\odot}$ disk. For this disk mass (corresponding to $E_T = 0.01M_{\odot}c^2$) the engine activity can last for hundreds of seconds if T_{\max} is sufficiently low (e.g., 15 MeV as in Fig. 5). In general, for a given M_{disk} , smaller T_{\max} imply smaller average energies released per episode (i.e. smaller accretion rates), and thus longer lifetimes.

We also note that the variability observed in the first few seconds of the $E_T = 0.01M_{\odot}c^2$ simulations is very similar to the $E_T = 0.001M_{\odot}c^2$ case which lasts for ~ 2 s, recall Figs. 3 and 4. Similarly, the variability seen in the first few seconds of a $E_T = 0.1M_{\odot}c^2$ simulation (not shown here) bears many similarities to the $E_T = 0.01M_{\odot}c^2$ case. This “self-similar” behavior is due to the duration being controlled by accretion timescales $\Delta t_{\text{accr}} > \Delta t_{\gamma}$, in connection with the stochastic accretion process whose main effect is to spread the events (peaks) randomly in time.

3.3. Total energy

In our model up to 10% of $M_{\text{disk}}c^2$ can be transformed into fireball energy. E.g., if an accretion disk with mass $0.1M_{\odot}$ surrounds a CFL star following its formation (see § 3.5), up to 10^{52} ergs of energy can be released in γ -rays. Larger disks lead to higher energy release but in this case the star is likely to become a black hole in the process.

3.4. Baryon loading and beaming

The intense, localised (source size < 100 km) and brief explosion implied by the observed GRB fluxes imply the formation of a e^+e^- -photon fireball. Furthermore, most of the spectral energy in GRBs is observed at ≥ 0.5 MeV, so the optical depth for $\gamma\gamma \rightarrow e^+e^-$ processes is very large. Any photon generated above 0.511 MeV will be degraded to below 0.511 MeV via the $\gamma\gamma \rightarrow e^+e^-$ process. This is the so-called compactness problem leading to a thermalised fireball (Ruderman 1975) unlike the optically thin spectra observed in GRBs.

The compactness problem can be resolved if the emitting matter is moving relativistically toward the observer. In this case the relative angle at which the photons collide must be less than the inverse of the bulk Lorentz factor, $1/\Gamma$, to effectively reduce the threshold energy for e^+e^- pair production (Goodman 1986). One can show that $\Gamma \geq 100$ is required to overcome the compactness problem (Shemi & Piran 1990; Paczyński 1990). This relativistic outflow presumably arises from an initial energy

E_0 imparted to a mass $M_0 \ll E_0/c^2$ close to the central engine (cf. Mészáros 2002 for more details).

The absence of electrons in CFL matter precludes the existence of a crust of normal matter around CFL stars, rendering them bare by construction (e.g., Lugones & Horvath 2003). In our model the emitted photons are likely to interact with particles from the accreting material. To enable acceleration to Lorentz factors above 100 the photon energy must be imparted on particles representing on average less than 0.1% of the total matter accreted per episode, since $\Gamma = \eta \dot{m}_{\text{acc}} c^2 \Delta t_{\text{accr}} / m_{\text{ejec}} c^2 = \eta (m_{\text{accr}} / m_{\text{ejec}})$. In other words, we require most of the infall material to convert to CFL matter with only a small portion of it to be ejected. This seems not unreasonable as most of the accreted particles will instantly deconfine to quark matter upon contact with the star's surface (see, e.g., Weber 2005).

The amount of mass ejected will vary from one episode to another leading to a spread in the Lorentz-factor distribution as already indicated in Figs. 3, 4 and 5. A fast loaded fireball that was injected after a slower one will eventually catch up and collide, converting some of the kinetic energy of the shells to thermal energy. This is reminiscent of the popular internal-shock model for GRBs (see, e.g., Kobayashi et al. 1997; Piran 2005) where a succession of relativistic shells collide and release the shock energy via synchrotron emission and inverse Compton scattering.

The intricate details of the accretion-ejection cycles are beyond the scope of this paper. Qualitatively, upon taking into account the star-disk magnetic field, we expect accretion to be channelled toward the polar regions as illustrated in Fig. 6. A refined scenario could further include hot bursting spots on the surface of the CFL star emitting γ -rays; the outgoing photons interact with the particles from the accreting matter ejecting part of it. Thus, in our model, the loaded fireballs emanate mostly from the polar regions with collimation reinforced by the magnetic field (e.g., Fendt & Ouyed 2004). When a hot spot cools below T_a , further accretion is triggered leading to another photon-bursting spot on the star as pictured in Fig. 6. The time delay between two successive spots is related to the randomness in the accretion (reheating) and the cooling timescales as described in § 3.1. This process continues until E_T is consumed, which in some cases can support up to hundreds of episodes (subjets), as in Fig. 5.

3.5. Formation scenarios/sites

In scenarios for the formation of CFL stars massive progenitors are naturally favoured since they are more likely to lead to compact remnants with high enough densities in the core for a (phase) transition to quark matter to occur. This is in line with afterglow observations which have provided several hints that some GRBs are associated with massive star progenitors (Galama et al. 1998, van Paradijs et al. 1999). If the quark star forms immediately following a supernova (SN) explosion of a massive progenitor,

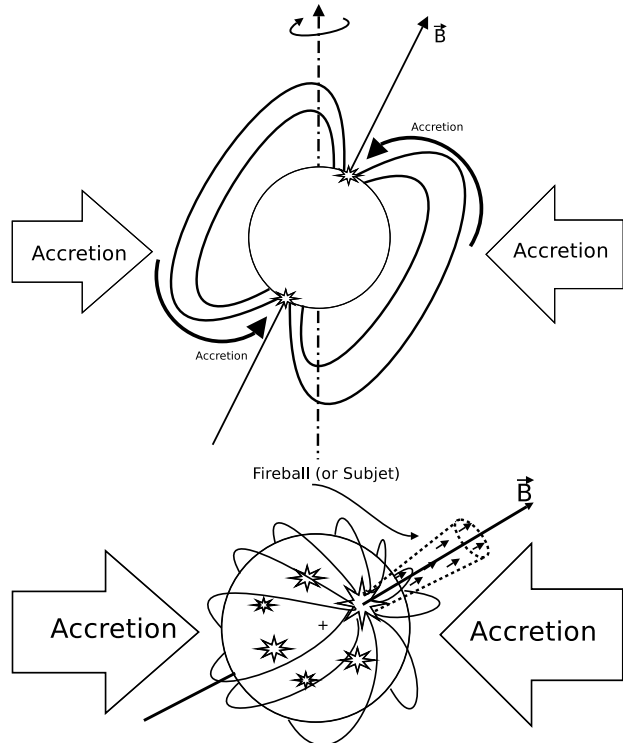


Fig. 6. Illustration of the intermittent accretion-ejection mechanism in our model. The upper panel shows the disk material channelled by the magnetic field toward the polar regions reheating the surface temperature to T_{peak} (the flashy spots). When $T_{\text{peak}} > T_a$, a photon burst is triggered ejecting particles from the accreting material. From a viewpoint along the polar axis (depicted by a cross in the lower panel), the multiple flashes on the surface of the star illustrate the locations of previous bursts (or ejections) induced by previous accretion episodes. The spatial spread of these flashes portrays the randomness in the accretion and cooling timescales.

a thick disk ($M_{\text{disk}} > 0.1 M_{\odot}$) is expected to form from fall-back material. The faster fireballs from the CFL star will catch up with the preceding supernova shell as to energise it. In fact, the energetic subjets from the CFL star are capable of destroying the original symmetry of the expanding SN shell. Another possibility involving massive progenitors is that of a collapsar-like event (Woosley 1993) where a quark star is formed instead of a black hole. In this scenario as well one would favour thick and massive disks to form around the star.

The hadron-quark transition may also happen long after the supernova explosion as in the Quark-Nova model where a neutron star (originally formed from a massive progenitor) can reach quark-matter densities through accretion from a companion, or due to spin-down (Ouyed, Dey, & Dey 2002; Ouyed et al. 2004). In some cases, the phase transition may take tens of millions of years to occur. During the explosion up to $0.01 M_{\odot}$ of material can be ejected (Keränen, Ouyed, & Jaikumar 2005) which later turns into a hyperaccreting disk (Keränen & Ouyed 2003).

3.6. Bimodality: Short and long duration GRBs

The durations of GRBs observed by BATSE show a bimodal distribution, which has led to a classification of GRBs into short (with $t_{90} < 2$ s, where t_{90} is the decay time to 10% intensity) and long ($t_{90} > 2$ s) (Kouveliotou et al. 1993; McBreen et al. 1994). It has been suggested that different underlying engines are operative, the short ones being related to binary neutron star mergers, and the long ones to the collapse of massive stars (see Mészáros 2002, and references therein). However, recent comparisons of short GRBs lightcurves to the first few seconds in long GRBs indicate that the two classes could be similar (e.g., Nakar&Piran 2002; Ghirlanda et al. 2004).

As noted in § 3.1, our model provides a kind of “self-similar” behaviour where the variability in the first few seconds of a long duration GRBs (thick disk) is reminiscent of that of a short GRB (thin disk), both driven by the same engine. As for the observed bimodality, it is possible that the formation scenarios discussed in § 3.5 (namely, collapsar-like events and Quark-Nova explosion) lead to 2 distinct classes of accretion disk (thick with $M_{\text{disk}} > 0.01M_{\odot}$ and thin with $M_{\text{disk}} < 0.01M_{\odot}$) surrounding the CFL star.

Interestingly, it has been argued recently in the literature that the bimodality in GRB duration originates from discrete emission regions (subjets) in the GRB jet (Toma, Yamazaki, & Nakamura 2005 and references therein). In this model the multiplicity of the subjets (n_s) along a line-of-sight differentiates between short GRBs ($n_s \sim 1$) and long GRBs ($n_s \gg 1$). Many subjets have to be randomly launched by the central engine for the model to work. This bears a close resemblance to the picture we developed here (cf. Fig. 5) and warrants more detailed studies of accretion-ejection within our model.

4. Conclusion

We have studied consequences of previously calculated photon (γ -ray) emission mechanisms in CFL matter for the early cooling of CFL stars. Based on the notion that pertinent emissivities essentially saturate the blackbody limit for temperatures $T \simeq 10\text{--}30$ MeV (due to underlying processes involving the Goldstone bosons of CFL matter), we have solved a diffusion equation and found that each photon burst can release an average energy of $\sim 10^{49}$ erg during a fraction of a millisecond. We have suggested a schematic model within which the time variability and the long activity (up to hundreds of seconds) of a GRB engine is driven by a surrounding hyperaccreting disk resulting from the formation process of the CFL star. This model reproduces several features of observed GRB spectra.

For a more quantitative description of the complex energetics and dynamics involved in our model, advanced numerical simulations should be performed accounting for general relativistic effects, as well as the star-disk magnetic field. Such studies will be similar to what has been done in the case of black-hole-accretion-disk systems (De

Villiers, Staff, & Ouyed 2005), with the black hole being replaced by a CFL star.

Acknowledgements. The research of R.O. is supported by grants from the Natural Science and Engineering Research Council of Canada (NSERC) and the Alberta Ingenuity Fund (AIF), and the research of R.R. is supported in part by a U.S. National Science Foundation CAREER award under grant PHY-0449489.

References

Alcock, C., Farhi, E., & Olinto, A. 1986, ApJ, 310, 261
 Alford, M., Rajagopal, K., & Wilczek, F. 1998, Phys. Lett. B422, 247
 Alford, M., Rajagopal, K., & Wilczek, F. 1999, Nucl. Phys. B537, 443
 Alford, M., Bowers, J.A., and Rajagopal, K. 2001, Phys. Rev. D63, 074016
 Alford, M., & Rajagopal, K. 2002, JHEP, 06, 31
 Alford, M. & Reddy, S. 2003, Phys. Rev. D67, 074024
 Buballa, M., Neuman, F., Oertel, M. & Shovkovy, I. 2004, Phys. Lett. B, 595, 36
 Chmaj, T., Haensel, P., & Slomiński, W. 1991, Nucl. Phys. B, 24, 40
 De Villiers, J. P., Staff, J., & Ouyed, R. 2005 [astro-ph/0502225]
 Frank, J., King, R., & Raine, D. J. 1992, Accretion power in astrophysics (Cambridge University Press)
 Frolov, V. P., & Lee, H. K. 2005, Phys. Rev. D, 71, 044002
 Galama, T. et al. 1998, Nature, 395, 670
 Ghirlanda, G., Ghisellini, G., & Celotti, A. 2004, A&A, 422, L55
 Glendenning, N. K. 1997, Compact stars (Springer)
 Goodman, J. 1986, ApJ, 308, L47
 Jaikumar, P., Prakash, M., & Schäfer, T. 2002 Phys. Rev. D, 66, 063003
 Keränen, P., & Ouyed, R. 2003, A&A, 2003, 407, L51
 Keränen, P., Ouyed, R., & Jaikumar, P. 2005, ApJ, 618, 485
 Kobayashi, S., Piran, T., & Sari, R. 1997, ApJ, 490, 92
 Kouveliotou, Ch. et al. 1993, ApJ, 413, L101
 Lugones, G., & Horvath, 2002, Phys. Rev. D66, 074017
 Lugones, G., & Horvath, J. E. 2003, A&A, 403, 173
 McBreen, B., Hurley, K. J., Long, R., & Metcalfe, L. 1994, MNRAS, 271, 662
 Mészáros, P. 2002 , ARA&A, 40, 137
 Nakar, E., & Piran, T. 2002, MNRAS, 330, 920
 Ouyed, R., & Sannino, F. 2001, Phys. Lett. B, 511, 66
 Ouyed, R., & Sannino, F. 2002, A&A, 387, 725
 Ouyed, R., Dey, J., & Dey, M. 2002, A&A, 390, L39
 Ouyed, R., Elgarøy, Ø., Dahle, H., & Keränen, P. 2004, A&A, 420, 1025
 Paczyński, B. 1990, ApJ, 363, 218
 Page, D. & Usov, V. V. 2002, Phys. Rev. Lett., 89, 131101
 Piran, T. 2000, Phys. Repor., 333, 529
 Piran, T. 2005, Rev. Mod. Phys. 76, 1143
 Popham, R., Woosley, S. E., & Fryer, Ch. 1999, ApJ, 518, 356
 Rajagopal, K. & Wilczek, F. 2000, in *At the Frontier of Particle Physics / Handbook of QCD*, Shifman, M. (ed.), World Scientific, vol. 3, 2061, and e-print hep-ph/0011333
 Rapp, R., Schäfer, T., Shuryak, E.V. & Velkovsky, M. 1998, Phys. Rev. Lett. 81, 53

Rapp, R., Shuryak, E.V., & Zahed, I. 2001, Phys. Rev. D63, 034008

Reddy, S., Sadzikowski, M., & Tachibana, M. 2002, Nucl. Phys. A, 714, 337

Ruderman, M. 1975, in 7th Texas Symposium on Relativistic Astrophysics, Tx., 1974, Ann. N.Y. Acad. Sci. 262, 164

Shemi, A., & Piran, T. 1990, ApJ, 365, L55

Shovkovy, I. A., & Ellis, P. J. 2002 Phys. Rev. C, 66, 015802

Toma, K., Yamazaki, R., & Nakamura, T. 2005, ApJ, 620, 835

Usov, V.V. 2001, ApJ, 550, L179

van Paradijs, J. et al. 1999, Science, 286, 693

Vogt, C., R., Rapp, & R. Ouyed 2004, Nucl. Phys. A, 735, 543 (VRO)

Weber, F. 2005, Prog. Part. Nucl. Phys., 54, 193

Woosley, S. E. 1993, ApJ, 405, 273